The Adsorption Behavior of Cu(II), Pb(II), and Co(II) of Ethylene Vinyl Acetate-Clinoptilolite Nanocomposites

T. S. Mthombo,[1] A. K. Mishra,[2] S. B. Mishra,[1] B. B. Mamba[1]

[1]*Department of Chemical Technology, University of Johannesburg, Doornfontein 2028, Johannesburg, South Africa*
[2]*UJ Nanomaterials Science Research Group, Department of Chemical Technology, University of Johannesburg, Doornfontein 2028, Johannesburg, South Africa*

Received 4 November 2010; accepted 5 December 2010
DOI 10.1002/app.34184
Published online 12 April 2011 in Wiley Online Library (wileyonlinelibrary.com).

ABSTRACT: In this study, ethylene vinyl acetate (EVA) was mixed with clinoptilolite (C), a natural zeolite, to prepare EVA-C nanocomposites. The films were characterized by SEM-EDS, XRD, and FT-IR, and heavy metal removal was studied using the batch technique. The effects of the initial pH value and concentration of solutions, contact time, and filler dosage on the adsorption capacity of the composites were investigated. To study the influence of pretreatment on the filler, clinoptilolite was activated using KCl, NaCl, and HCl. Adsorption results show that equilibrium was reached after 24 h, and that sorption reached its maximum at pH values between 5 and 7. The selectivity trend was observed to be Pb > Cu > Co, which was consistent for both single and mixed metal-ion solutions. Pretreatment significantly increased adsorption capacity of the composite, but was dependent on the conditioning reagent. Nanocomposites filled with HCl-activated particles demonstrated a high adsorption capacity of between 70 and 80% for all three metals, while KCl-activated particles were the least efficient with a maximum adsorption capacity of 69% for Pb(II), 54% for Cu(II) and 48% for Co(II). The adsorption data were then fitted to both Langmuir and Freundlich isotherms over the entire concentration range, and the Langmuir isotherm showed a better fit of the experimental sorption data than the Freundlich isotherm. The results obtained show that this simple methodology which can be up-scaled has great potential for the preparation of a wide variety of similar particle-filled adsorbent nanocomposites in other environmental remediation applications. © 2011 Wiley Periodicals, Inc. J Appl Polym Sci 121: 3414–3424, 2011

Key words: clinoptilolite; EVA; nanocomposites; adsorption; heavy metals

INTRODUCTION

Lead, copper and cobalt ions are among the most hazardous inorganic pollutants found in heavy-metal-laden water systems, and are generated by industrial activities such as mining, petroleum refining, electroplating, and the textile industry. The presence of these cationic species in aquatic ecosystems results in their accumulation in living organisms, which causes several adverse effects. For example, Pb^{2+} interacts with the sulfhydryl group in human protein and also impairs the synthesis of hemoglobin, resulting in severe disruptions in the metabolism and function of the brain, liver, and kidneys.[1] In plants, Pb^{2+} tends to accumulate within the cell walls and intermolecular spaces, resulting in plant growth retardation.[2] Cobalt, on the other hand, has been implicated in dermatitis and in affecting the respiratory system, while vomiting and nausea are some of the symptoms of Cu^{2+} poisoning.[3,4] For these reasons, the remediation, treatment, and removal of heavy-metal ions from water have become a major concern for many processing industries.

Several techniques, including chemical coagulation, membrane separation, ion exchange, ultrafiltration, and adsorption have been developed for water treatment. Many of these methods may, however, prove to be less effective than required and they generate secondary pollution with intermediates such as sludge. Adsorption has attracted much interest among researchers due to its low energy requirements and effectiveness even at low concentrations.[5] Activated carbon has been the most widely used adsorbent due to its effective metal-ion adsorption and its relatively high mechanical properties.[6] However, the high cost of the process of activation is a major limitation for use in water treatment, especially in developing countries, hence the need for the development of low-cost adsorbent materials. Natural minerals such as clays, zeolites, fly ash, and biomass are typical low-cost adsorbents.[7] Zeolites in particular have been intensively studied because of their ability to remove trace quantities of heavy metal

Correspondence to: A. K. Mishra (amishra@uj.ac.za).
Contract grant sponsors: DST/Mintek Nanotechnology Innovation Centre (NIC); National Research Foundation (NRF); University of Johannesburg (UJ).

ions by utilizing the ion-exchange phenomenon. Zeolites are naturally occurring crystalline aluminosilicates consisting of a framework of tetrahedral molecules linked to each other by corner-sharing oxygen atoms. Each Al^{3+} substitution for Si^{4+} results in a deficiency of positive charges within the framework. The negative charges are then balanced by positively charged cations such as Na^{+}, K^{+}, Ca^{2+}, and Mg^{2+} on the pore surface of the microporous structure.[8] These cations are coordinated with the defined number of water molecules, and are bound to the aluminosilicate framework by weaker electrostatic bonds, enabling ion exchange with the cations in solution.[9] Clinoptilolite, the most abundant zeolite, has generated much interest among scientists due to its high ion-exchange capacity and selectivity for divalent sorbates. It is also very stable in terms of dehydration and has a high thermal stability of 700°C in air, the highest of all other natural zeolites with a similar structure.[8,10] Moreover, on the basis of adsorbent mass, clinoptilolite as an adsorbent has a larger surface area than bulk particles and can be pretreated with various conditioning agents (acids, bases, surfactants, etc.) to increase its affinity for targeted compounds. Pretreatment is aimed at replacing exchangeable cations on the pore surface with a cation that is more willing to undergo cation exchange with ions in solution.[11,12] However, the use of clinoptilolite in powder form at nanoscale is a major limitation. The aggregation of particles under different electrolytes leads to variations in the flow properties of the mineral, and this is an undesired feature for their use as sorbents. Therefore, it becomes imperative to incorporate particular additives to counter-act this characteristic behavior. In particular, incorporation of polymers enables the application of the mineral itself as an adsorbent confined in an isolated and practically usable medium in aquatic systems.[13]

In this study, ethylene vinyl acetate (EVA), a copolymer of ethylene and vinyl acetate, has been mixed with clinoptilolite (C) as the filler, to prepare EVA-C nanocomposites. Although non-biodegradable, EVA is an inert, hydrophilic polymer with excellent cohesive strength and adhesion to a wide range of substrates. Incorporation of the clinoptilolite, with its high mechanical and chemical resistance, into the polymer matrix yields an effective adsorbent and ion-exchange medium that has the potential to combine the advantages of both while eliminating their shortcomings. The present study investigates the applicability of the EVA-C nanocomposite for the sequestration of Cu^{2+}, Pb^{2+}, and Co^{2+} from aqueous solutions. The influence of factors such as pH, contact time, initial concentration of solutions, and pretreatment of the filler was investigated and the results are presented here. Sorption mechanisms of the metal ions in single and mixed solutions are also discussed.

EXPERIMENTAL

Materials

The clinoptilolite used in this study was supplied by Pratley South Africa and was sourced from the Vulture Creek in the KwaZulu-Natal Province of South Africa. EVA is a commercial product and was supplied by Plastamid, South Africa. $Pb(NO_3)$, $CuSO_4{\cdot}5H_2O$ and $CoSO_4{\cdot}7H_2O$ were used as metal-ion sources while NaCl, KCl, and HCl were used as conditioning reagents. All reagents were of analytical grade of the highest purity available, and were supplied by Sigma Aldrich and Merck.

Characterization of clinoptilolite

Particles of the original ("as-received") clinoptilolite were ground and sieved with the 38-μm sieve, then washed with deionized water and dried at 105°C overnight. To investigate the effect of chemical conditioning, three conditioning reagents, NaCl, KCl, and HCl were used. The clinoptilolite particles were soaked in 2*M* solutions of each reagent and shaken for 72 h after which the particles were washed with deionized water to remove traces of the anions followed by drying at 105°C for 24 h. The morphology and chemical composition of the zeolite particles were determined by scanning electron microscopy-energy dispersive spectroscopy (SEM-EDS), using a Jeol JSM 5600. Fine particles were mounted on a carbon tape and coated with carbon to induce conductivity. The samples were then introduced into a vacuum cell to obtain micrographs of the zeolite. SEM-EDS measurements were carried out to compare the chemical composition of the "as-received" and the conditioned forms of the samples. Chemical composition was determined by X-ray powder diffractrometry (Phillips X'pert), with Cu Kα scanning from $2\theta = 4^{\circ}$ to 80°, while bulk analyses were carried out by X-ray fluorescence (XRF) spectroscopy using a Phillips Magix Pro. Surface area analysis was done using the Brunauer-Emmett-Teller (BET) method with an automated gas adsorption analyzer (Micromeritics ASAP 2020). Samples were first degassed (cleaned) under nitrogen atmosphere for 6 h at 150°C at an N_2 flow rate of 60 mL min^{-1}.

Preparation of EVA-C nanocomposites and characterization

All EVA-C nanocomposites were prepared by the melt-mixing technique in a rheomixer (Haake Rheomex OS) at 120°C and at a speed of 60 r min^{-1} for 30 min. The mass of polymer or filler required for specific ratios ranging between 100 : 0 and 70 : 30 (polymer : zeolite) was calculated using the "mixing" equation below:

$$m = \rho \times V_c \times f \times W_t \quad (1)$$

TABLE I
Chemical Composition from the Bulk Analysis (XRF) of Both the "As-Received" (A.R.) and Chemically Conditioned Clinoptilolite

	% Abundance		
Composition	A.R. Clinoptilolite	Na^+ -clinoptilolite	K^+ -Clinoptilolite
Al_2O_3	12.42	12.62	12.49
CaO	1.29	0.31	0.14
Cr_2O_3	–	–	–
Fe_2O_3	1.22	0.42	0.17
K_2O	3.77	2.62	10.08
MgO	0.87	0.35	–
MnO	–	–	–
Na_2O	1.31	5.31	–
P_2O5	–	–	–
SiO_2	71.37	71.11	70.62
SO_3	–	–	–
TiO_2	0.14	0.15	0.15
LOI (at 930°C)	6.9	6.5	5.7
Total	99.29	99.13	99.23

LOI = loss on ignition.

where m is the mass (g), ρ is the density of polymer (or clinoptilolite), V_c and f are constants for the chamber volume and filler rate of the rheomixer, respectively, Wt (%) represents the required weight of polymer or filler.

The composite strips were then extruded through a single-screw extruder at 120°C to obtain strips with an average width of 0.5 mm, and the films were characterized with SEM-EDS and XRD. Fourier Transform Infrared (FT-IR) spectroscopy was also carried out to ascertain the effect of pretreatment, which should have an effect on the overall adsorption efficiency of the adsorbent composites.

Adsorption studies

The sorption behavior of the three metals on the adsorbent composite was studied using the batch technique at room temperature. Synthetic stock solutions of Pb^{2+}, Cu^{2+}, and Co^{2+} were prepared by dissolving $Pb(NO_3)_2$, $CuSO_4{\cdot}5H_2O$, and $CoSO_4{\cdot}7H_2O$ in 1000-mL volumetric flasks, respectively, then diluted accordingly to generate the required concentrations. To investigate the effect of competing cations, mixed solutions were prepared by varying the concentrations of ions in solution in the ratios 1 : 1 : 1, 2 : 1 : 1, and 1 : 1 : 2 for Pb^{2+}, Cu^{2+}, and Co^{2+}, respectively. In all experiments throughout the study, adsorbent strips of 40 mm × 20 mm length were placed in 50 mL of the synthetic solution during adsorption studies. All solutions were analyzed within 24 h to eliminate errors emanating from container plating or precipitation of the metal ions. Metal-ion content was quantified using atomic absorption spectroscopy (GBS Avanta 1.33) using an air-acetylene flame. All experiments were conducted in triplicate and mean values were used. The metal uptake degree (α) and the adsorbed metal amount per volume (q) were calculated as follows:

$$\alpha = \frac{C_i - C_f}{C_i} \times 100\% \quad (2)$$

$$q = \frac{C_i - C_f}{C_i} \times \frac{V}{m} (\mathrm{mg/g}) \quad (3)$$

where m is the mass of the adsorbent composite strip, V is the volume of the solution, C_i and C_f represent the initial and final concentrations, respectively

RESULTS AND DISCUSSION

Characterization of clinoptilolite

The chemical analyses of the original clinoptilolite are given in Table I. The zeolite contained calcium, potassium, sodium, and magnesium as exchangeable cations as well as titanium in trace amounts. The effect of NaCl and KCl conditioning is illustrated by the increase in percentage abundance of the NaCl and K_2O metal oxides, respectively. From this composition, the Si/Al ratio was calculated as 5.6, which is within the acceptable characteristic range for clinoptilolite.[14]

Table II shows comparative data of the physical properties of both the original clinoptilolite and the pretreated samples. These data suggest that pretreatment greatly improves the surface area and pore volume as the conditioning opens the channels and pore openings within the framework, initially clogged by fine dust particles produced during crushing of the clinoptilolite.[15] HCl-activated particles presented the greatest surface area, which should have an influence on the adsorption capacity of the nanocomposites filled with HCl-activated clinoptilolite. It has been reported in the literature that acid activation of natural clinoptilolite improves its sorption properties in ion-exchange processes due to the dissolution of amorphous silica fragments blocking the channels.[16]

The surface morphology of the original as well as chemically-conditioned clinoptilolite samples is shown in Figure 1. A significant change in the

TABLE II
A Comparison of the Physical Properties of A.R. Clinoptilolite and that Treated with KCl, HCl, and NaCl

Parameter	A.R.	HCl	NaCl	KCl
Specific surface area ($m^2\ g^{-1}$)	15.96	20.24	19.50	16.44
Pore volume ($cm^3\ g^{-1}$)	0.663	0.061	0.063	0.069
Average density ($g\ cm^{-3}$)	1.227	1.227	1.227	1.227

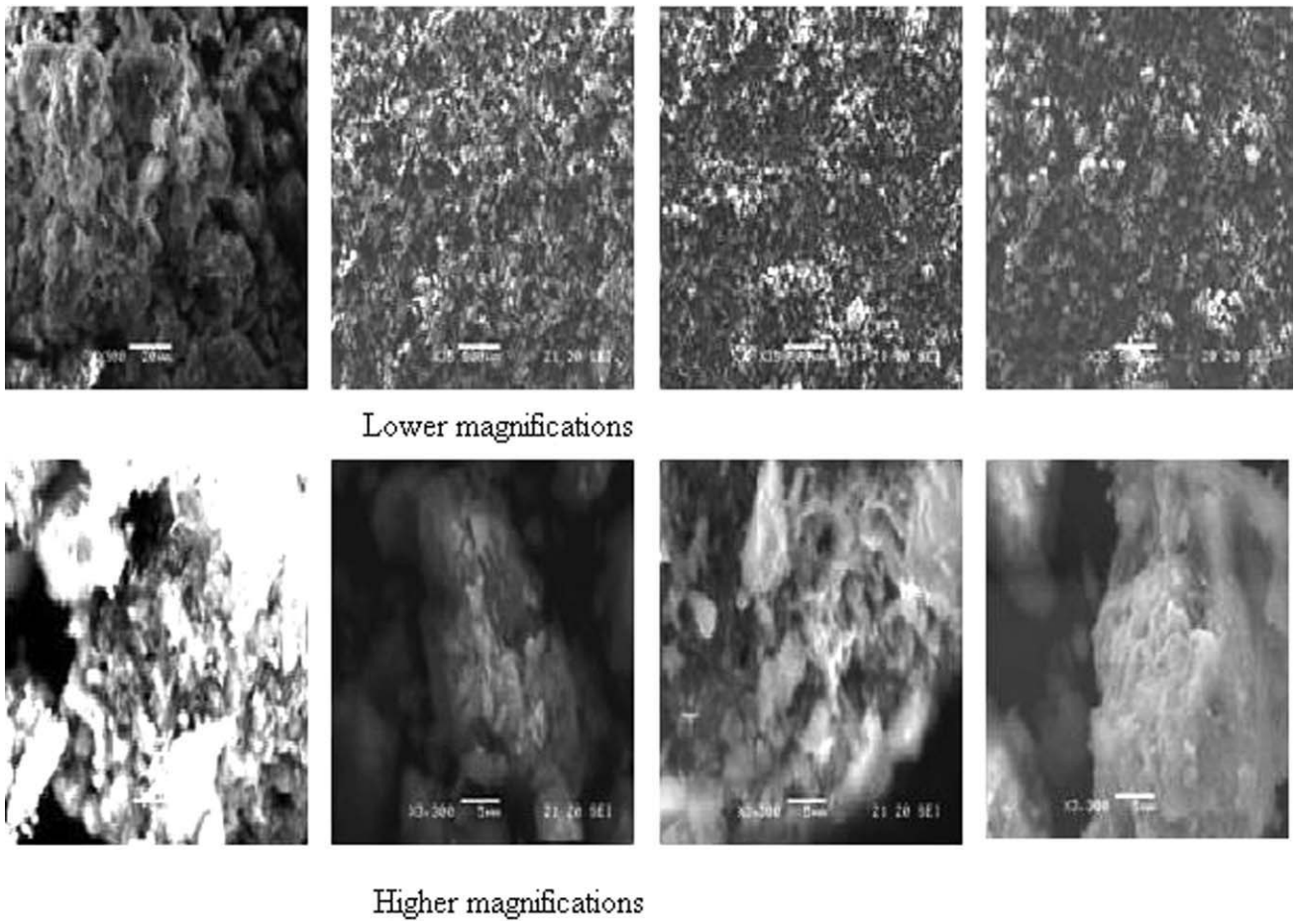

Figure 1 SEM micrographs of "as-received" clinoptilolite as well as KCl-, NaCl- and HCl-activated particles at (a) low magnification (×30) and (b) higher magnification (×3300).

morphology is observed between the "as-received" (a.r.) and chemically conditioned clinoptilolite particles at higher magnification. It is evident that conditioning softens the material and opens up the surface area producing "flake-like" structures (indicated with an arrow) for HCl-activated samples, when compared to the "rough and compact" structure of the original form.

Powder diffraction measurements of the particles also confirmed clinoptilolite as the main components with quartz and sadinine as the major impurities. A typical diffractometer pattern is shown in Figure 2. The main peaks at $2\theta = 9°$, 22°, and 30° are typical of clinoptilolites from the heulandite family.[14] For a comparative study of the effect of conditioning, an XRD pattern for NaCl and HCl-activated clinoptilolite is also shown in Figure 2. There seems to be no alteration in the crystal lattice of the zeolite, which shows that conditioning is nondestructive, but only involves the exchange of ions within the zeolite framework into a homoionic form. Studies by Hernandez[17] confirm the findings in this study with respect to the effect of chemical conditioning.

Characterization of EVA-C nanocomposites

In Figure 3 the SEM micrographs of the surface morphology of plain EVA as well as clinoptilolite-filled EVA are shown. The EVA copolymer has a uniform

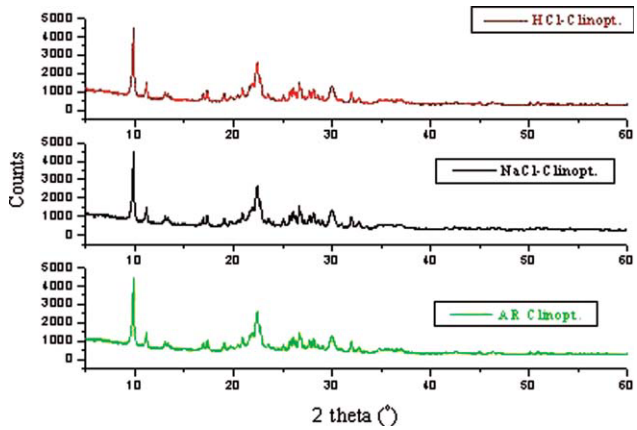

Figure 2 XRD patterns for "as-received" clinoptilolite in comparison with NaCl- and KCl- activated clinoptilolite samples. [Color figure can be viewed in the online issue, which is available at wileyonlinelibrary.com.]

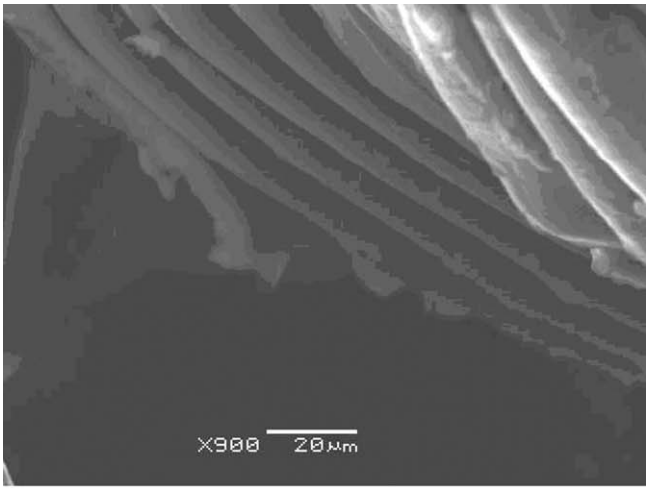

(a)

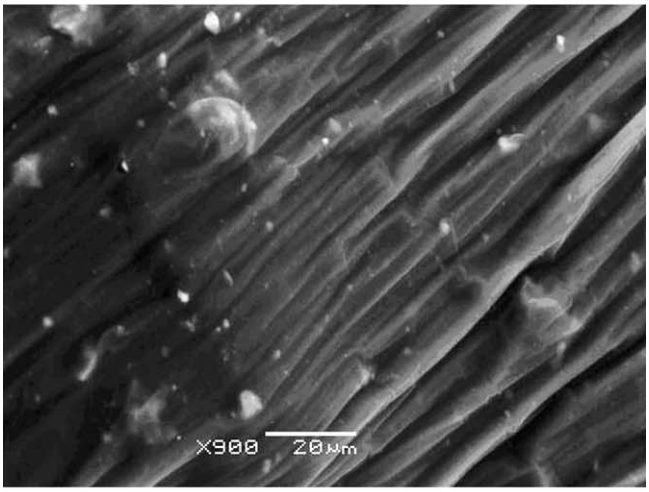

(b)

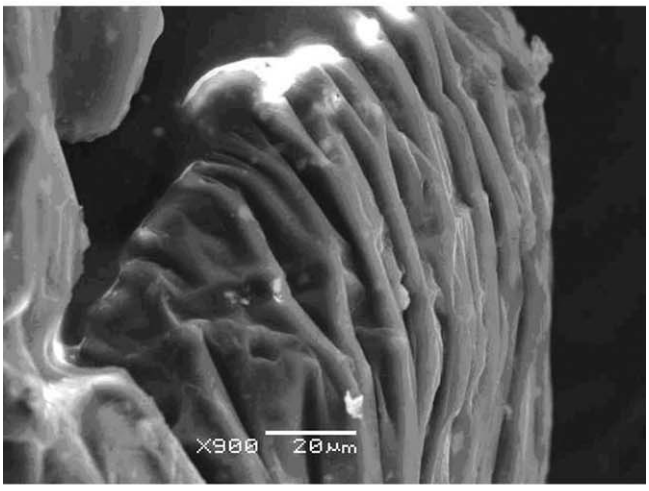

(c)

Figure 3 Surface morphology of (a) plain EVA, (b) EVA-C filled with 5% A.R clinoptilolite, and 10% in (c). The arrow in (c) shows a void formed as a result of particle agglomeration.

structure with characteristic "folds" [Fig. 3(c)]. However, this uniform structure appears to be "distorted" with increasing clinoptilolite dosage, a condition which perhaps is due to some degree of physical interaction between the polymer and the filler. Although the particles were sieved through a 38-μm sieve, agglomerates of the zeolite particles (spherical particles) are visible within the EVA matrix, perhaps due to interface incompatibility between the matrix and the filler phases, leading to voids being formed around the zeolite particles, as seen in Figure 3(c).

Figure 4 shows an SEM-EDS image of the surface of an EVA-C composite strip filled with 5% of the filler, which confirms the incorporation of clinoptilolite into the polymer matrix, as evidenced by the presence of the Al and Si peaks which are characteristic of the zeolite.

XRD patterns of the EVA-C composites are shown in Figure 5, and for the purposes of comparison, a typical XRD pattern for clinoptilolite is also included. Characteristic peaks of clinoptilolite are observed, further confirming the successful incorporation of the filler into the polymer matrix. Quartz is present as an impurity, and its presence was also confirmed in the original clinoptilolite. Furthermore, observations reveal that with increasing clinoptilolite loading in the composite, the spacing at the base of the peaks slightly increases and there is a slight shift of the peaks at $2\theta = 21$ to lower 2θ values, suggesting that the ordered framework of the zeolite is disrupted due to intercalation with the polymer.[18]

In Figure 6, the IR spectra of AR clinoptilolite and EVA/C composites filled only with the original clinoptilolite are shown. The stretching between 1500 and 1000 cm^{-1}, which is characteristic of zeolitic minerals, is not observed in the plain EVA. The strong IR band at 1001 cm^{-1} is characteristic of all forms of clinoptilolite, and is representative of the Si—O stretching.[19] An increase in intensity of this broad band is observed for the EVA-C composite filled with 30% (wt) of the filler, which is indicative of an increased concentration of filler particles. The peak at 1636 cm^{-1} indicates the presence of molecular water in the clinoptilolite sample. For the plain EVA the broad bands in the range 2800–2900cm^{-1} can be attributed to the stretching vibrations of —CH_3 and —COOH groups, whereas C=O stretching vibrations are in the range 1400–1700 cm^{-1}.[16]

Adsorption studies

Effect of clinoptilolite loading

The effect of sorbent dose (5–30 wt %) on the percentage removal of Pb^{2+}, Cu^{2+}, and Co^{2+} ions is

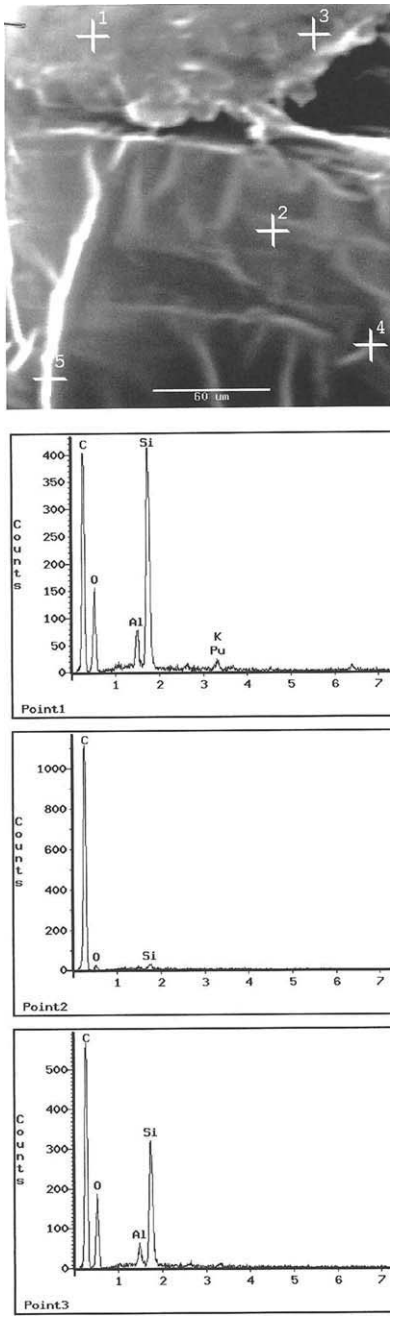

Figure 4 SEM-EDS images showing the morphology of "as received" filled EVA-C (90–10 wt %), which confirms the presence of clinoptilolite in the nanocomposites.

shown in Figure 7. For all metal ions, the removal efficiency increases with an increase in the amount of clinoptilolite in the composite. This suggests that increasing the loading of the adsorbent filler also increases the surface area and hence the number of adsorption sites available in the composite films. However, as shown in Figure 7, the amount of metal removed per unit weight of the adsorbent q decreases at higher dosages. Maximum adsorption was attained at 15 and 20 wt % of the filler for Pb and Cu, respectively. This could be attributed to the

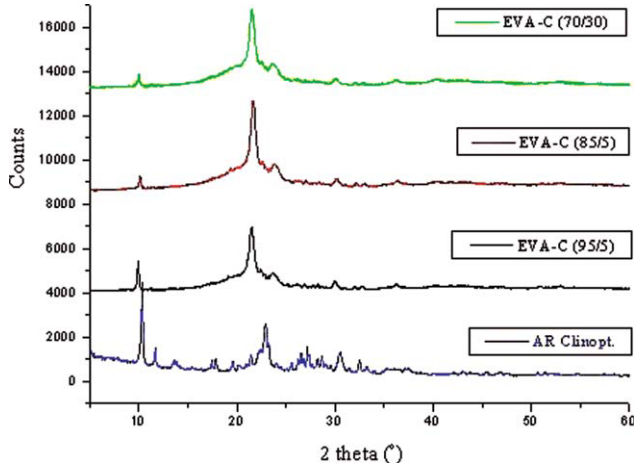

Figure 5 XRD patterns of EVA-C composites filled with 5 and 10% of the filler as well as that of the original clinoptilolite. [Color figure can be viewed in the online issue, which is available at wileyonlinelibrary.com.]

fact that at higher adsorbent dose, the concentration of the ions in solution decreases hence the system reaches equilibrium at lower values of q, suggesting that some adsorption sites within the adsorbent composite remain unsaturated.[20]

Effect of contact time

The effect of contact time on the metal-ion retention capacity was studied by varying the time from 0 to 48 h, at a fixed initial concentration of 10 mg L^{-1}, and the results are presented in Figure 8. With all the metal ions, adsorption increased over time, and equilibrium was reached after 24 h. This could be attributed to saturation levels being attained at active sites. All subsequent batch experiments were then carried out over the equilibrium time of 24 h.

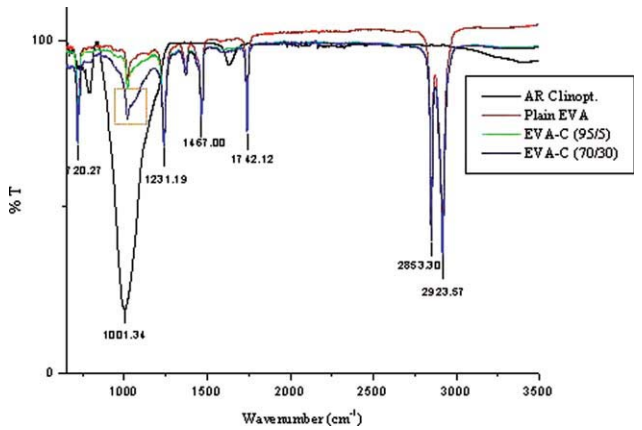

Figure 6 The IR spectra of plain EVA as well as those of "as received" filled EVA-C composites. [Color figure can be viewed in the online issue, which is available at wileyonlinelibrary.com.]

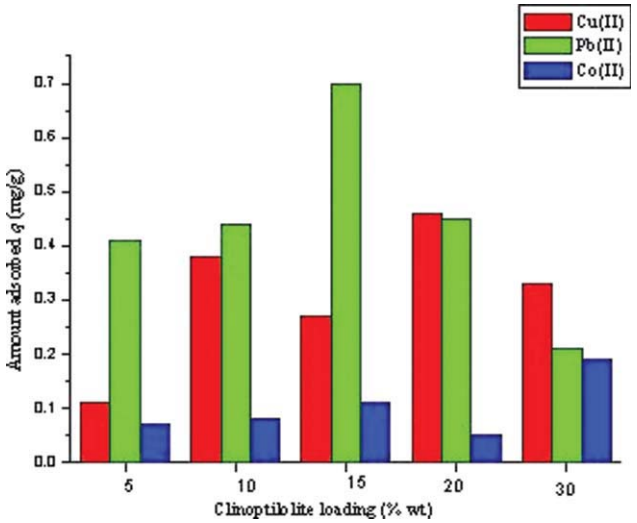

Figure 7 Adsorption studies of Pb, Cu, and Co onto EVA-C composites with varying filler dosage (5–30 wt %) at room temperature. [Color figure can be viewed in the online issue, which is available at wileyonlinelibrary.com.]

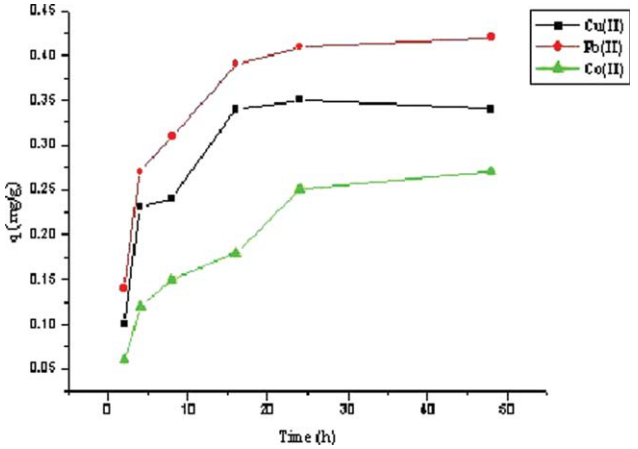

Figure 8 Adsorption of Pb^{2+}, Co^{2+}, and Cu^{2+} onto A.R-EVA/C (85/15 wt %) as a function of time. [Color figure can be viewed in the online issue, which is available at wileyonlinelibrary.com.]

Influence of pretreatment

To investigate the influence of pretreatment, composites filled with "as-received" clinoptilolite were compared with nanocomposites filled with NaCl-, HCl-, and KCl-activated particles. As seen in Figure 9, pretreatment improves the adsorption efficiency of all three metal ions, compared to the composites filled with untreated clinoptilolite. However, this improvement is also a function of the conditioning reagent in the order HCl > NaCl > KCl, and this can be explained as follows: acid (HCl) activation of natural clinoptilolite improves its ion-exchange capacity due to the dealumination, decatination, and dissolution of amorphous silica fragments blocking the channels.[14,21] The relatively lower adsorption capacity shown by KCl-activated composites could be due to the resilience of K^+ to participate in ion exchange as compared to Na^+. This behavior is attributed to sites on the zeolite that are occupied by K^+. It is proposed that K^+ is located at a specific M(3) site which is situated in an eight-member ring and has the highest coordination among all the cationic sites in the unit cells, resulting in strong bonding. Thus KCl-activated zeolite would have a higher proportion of K^+ moieties on the lattice, which will in turn determine the cation-exchange capacity. These observations are in accordance with research work done and published by Cincotti et al.[22]

The effect of initial concentration

The adsorption of Co^{2+}, Pb^{2+}, and Cu^{2+} as a function of their initial concentrations was studied at 25°C by varying the metal concentration from 0.5 to 20 mg L^{-1} while keeping all other parameters constant, and the results are shown in Figure 10. As observed in Figure 10(a), the percentage adsorption of the three metal ions decreases with increasing metal concentration in solution. These results indicate that with increasing metal concentration adsorption sites that are less favorable in terms of energy levels become involved.[23] In Figure 10(b), the amount of metal ion adsorbed per volume (q) is plotted as a function of the initial concentration. From these results, it is observed that adsorption of ionic species occurs in two phases: an initial rapid phase and a slower second phase, during which the contribution to the total adsorption is relatively slow. The first phase is predominantly external surface adsorption while in the second phase

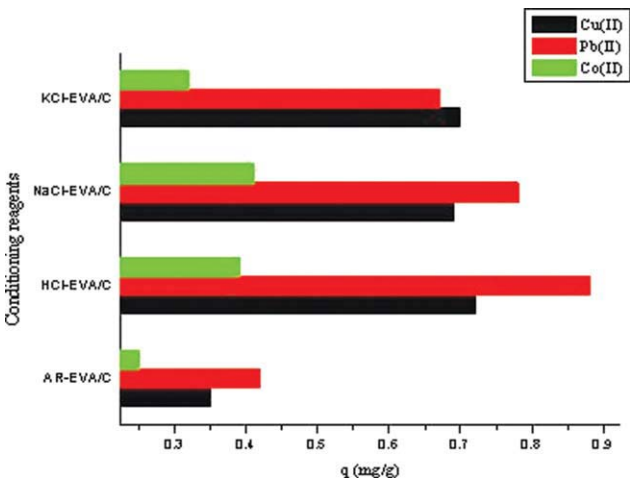

Figure 9 The influence of different conditioning reagents on the heavy metal uptake onto EVA-C(90-10) after 24 h, at room temperature. [Color figure can be viewed in the online issue, which is available at wileyonlinelibrary.com.]

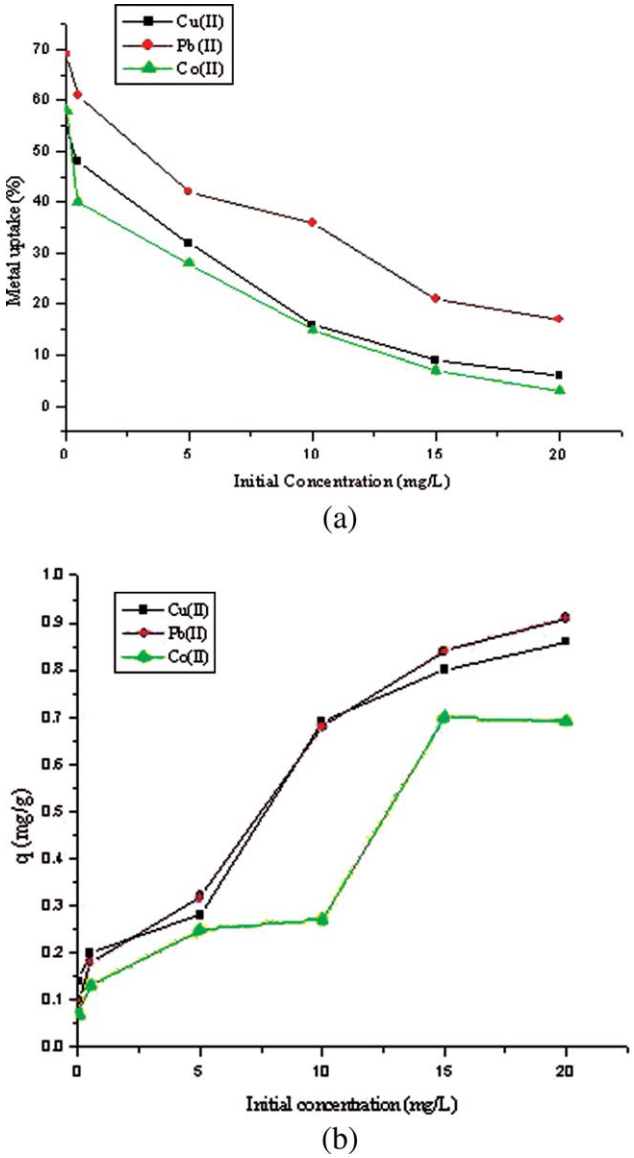

Figure 10 The percentage metal removal (α) is plotted in (a) while in (b), the amount adsorbed per unit mass of the adsorbent (q) is plotted as a function of the initial metal-ion concentrations, to illustrate adsorption behavior on NaCl-EVA/C after 24 h. [Color figure can be viewed in the online issue, which is available at wileyonlinelibrary.com.]

adsorption seems to be controlled by intraparticle diffusion processes.[24] The rapid cation uptake at low initial concentration is due to the fact that there are more exchangeable sites available in the adsorbent at low M^{2+}/adsorbent ratios (M^{2+} = metal cation), while, as the ratios increase, exchangeable sites become saturated resulting in a decrease in the rate of adsorption.[25]

Influence of pH

The ability of the EVA-C composite to adsorb Pb^{2+}, Co^{2+}, and Cu^{2+} was found to depend strongly on the pH of the sample solution. The pH was investigated at values ranging between pH 2 and 12, at a fixed solution concentration of 5 mg L^{-1}, and the results are depicted in Figure 11. The initial solution pH was set at less than pH 6 for all metal ions taking into account possible metal precipitation. With increasing pH levels, metal-ion uptake increased initially, reaching a maximum level at between pH 4 and 5 for Pb^{2+} and Cu^{2+}. For Co $^{2+}$ on the other hand, a maximum level was attained at pH 7. The solution pH affected both the carboxyl group (in EVA) of the adsorbent as well as competition for the binding sites by the cations. The formation of aqua-metal species and hydroxo-complexes is determined by the solution pH value.[26] At very low pH levels, the number of H_3O^+ significantly exceeds that of metal ions, and the latter cannot effectively compete with the H_3O^+ ions for the binding sites on the adsorbent. By increasing the pH, the surface charge of the adsorbent becomes more negative as the H_3O^+ concentration decreases and some sites become available to the metal ions. As the acidity decreases even further, more H_3O^+ ions on the surface of the adsorbent are replaced by metal ions such as Cu^{2+}, $Cu(OH)^+$; Pb^{2+}, $Pb(OH)^+$; and Co^{2+}, $Co(OH)_2$.[27–29]

Effect of competing cations

To investigate the effect of competitive adsorption, mixed solutions of the same and varying concentrations were compared. The results are presented in Figure 12. Heavy metal uptake is attributed to the diverse complex mechanisms of ion-exchange and adsorption processes. During the ion-exchange

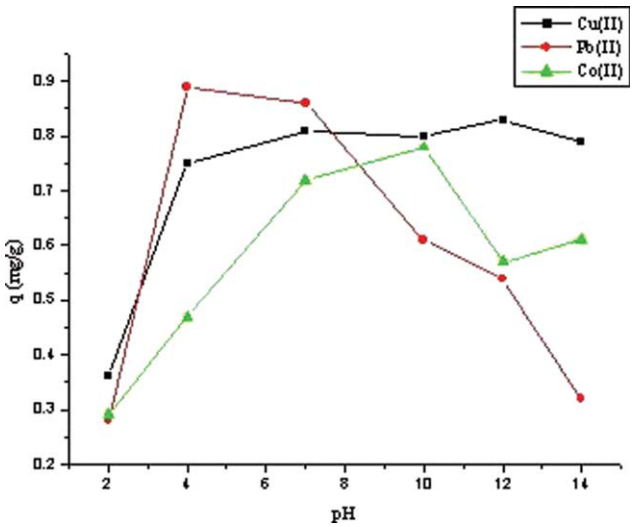

Figure 11 Influence of pH on the adsorption of Pb(II), Co(II), and Cu(II) onto HCl-EVA/C. [Color figure can be viewed in the online issue, which is available at wileyonlinelibrary.com.]

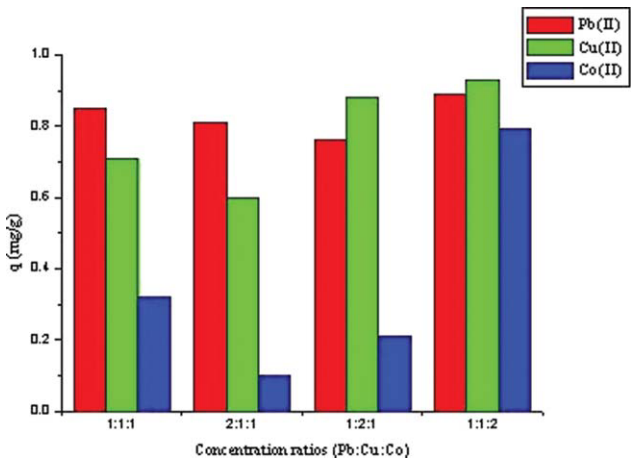

Figure 12 Competitive adsorption of the heavy metals at the same and varying concentrations. The ratios refer to the concentrations of Pb(II) : Cu(II) : Co(II), respectively, (pH = 6; t = 24 h). [Color figure can be viewed in the online issue, which is available at wileyonlinelibrary.com.]

process, metal ions move through the pores and channels of the zeolite, to replace exchangeable ions. Diffusion was faster through the pores and was retarded when ions moved through the smaller diameter channels of the microporous mineral. The adsorption phenomenon depends on the charge density of cations hence the diameter of the hydrate ions becomes important. Since the charges of all the cations studied are the same (+2), metal ions with the largest diameter will have minimum adsorption while those with the least diameter will have maximum adsorption.[23] As seen in Figure 12, Pb^{2+} is the most preferred cation while Co^{2+} is the least adsorbed. Thus the selectivity sequence is in the order: $Pb^{2+} > Cu^{2+} > Co^{2+}$, which is in accordance with the results obtained by Wang et al.[29] These findings can be attributed to the dissimilar preferences of the clinoptilolite for the various metal cations. Because of its high Si/Al ratio, clinoptilolite has a low charge density. Therefore, divalent cations with low hydration energies are sorbed preferentially compared to cations with high hydration energies. Thus a high concentration of Pb, with the lowest hydration energy, is expected to limit the uptake of Co and Cu. Competitive adsorption of the different metal ions at varying concentration ratios is also illustrated in Figure 12.

The phenomenon of one ion being favored over the other for ion exchange in mixed solutions is explained in terms of both the physicochemical and stereochemical factors, which include the hydration enthalpy of the cations, the radius of the ions, as well as the space requirements of the micropores within the adsorbent framework.[15] Metal cations in solution have characteristic hydrated layers of a defined stability. Ions with large radii will therefore be less favored by exchangers compared to ions with small radii. This explains why Cu^{2+}, with a smaller radius than Co^{2+}, is favored by the adsorbent even at higher concentrations of the latter. A significantly high amount of Co(II) was adsorbed at a higher concentration of Co (1 : 1 : 2). This suggests that both Pb^{2+} and Cu ions were involved in the formation of a relatively stable complex, and were not readily available for ion exchange, as they slowly dissociated from their Cu-Pb complex, as dictated by their dynamic equilibrium.[30]

Adsorption isotherms

The adsorption data were fitted to the Langmuir and Freundlich isotherms. The Langmuir isotherm holds true for monolayer adsorption due to a surface area of a finite number of identical sorption sites, and can be expressed in linearized form as:

$$C_e/q_e = b/Q_o + C_e/Q_o \quad (4)$$

where C_e is the equilibrium concentration (mg L^{-1}), q_e is the amount adsorbed at equilibrium, Q_o and b are Langmuir constants representing the adsorption capacity (mg g^{-1}) and the heat of adsorption, respectively

Also important in the Langmuir isotherm studies is a constant, R_L, a parameter which predicts whether an adsorption system is favorable or not, and is calculated as:

$$R_L = 1/1 + bC_o \quad (5)$$

where, C_o is the initial concentration (mg L^{-1}). For $0 < R_L < 1$ adsorption is favored, and the higher the value of R_L, the greater the favorability.[31]

The Freundlich isotherm describes the heterogeneous surface energies by multilayer adsorption and is expressed in linear form as:

$$\mathrm{In}q_e = \mathrm{In}K_f + n\ \mathrm{In}C_e \quad (6)$$

where, q_e is representative of the adsorption capacity (mg g^{-1}), n is an empirical parameter related to the intensity of adsorption.

TABLE III
Langmuir and Freundlich Isotherm Parameters for Pb(II), Cu(II), and Co(II) Adsorption by HCl-EVA/C (85/15)

	Langmuir model				Freundlich model		
M^{2+}	R^2	Q_0	R_L	b	R^2	K_f	n
Pb	0.912	0.982	0.865	0.310	0.895	0.410	1.055
Cu	0.956	0.870	0.791	0.528	0.882	0.288	0.793
Co	0.910	0.717	0.865	0.310	0.887	0.139	0.776

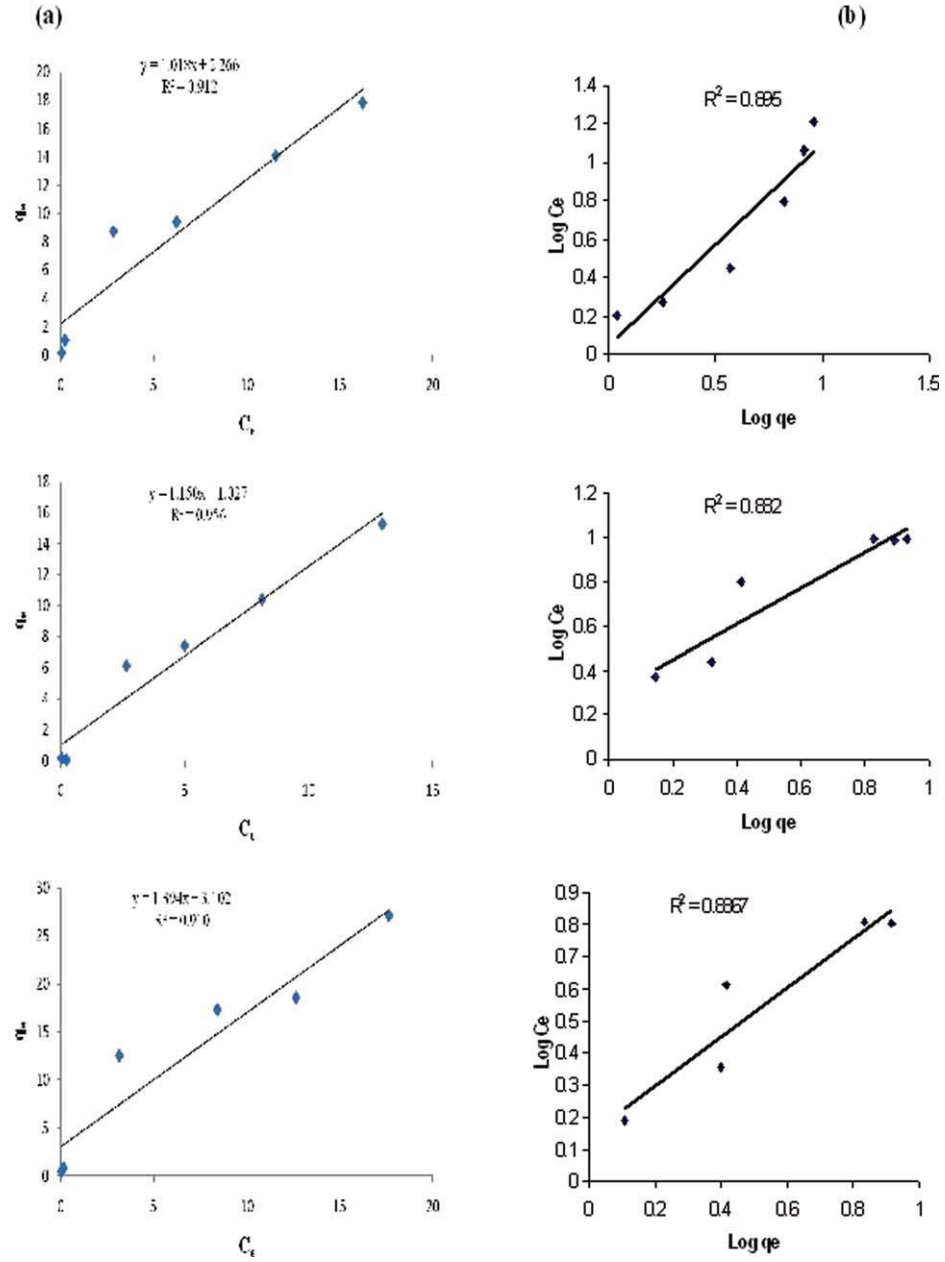

Figure 13 Langmuir (a) and Freundlich (b) adsorption isotherms for Pb(II), Cu(II), and Co(II) by HCl-EVA/C (85/15). [Color figure can be viewed in the online issue, which is available at wileyonlinelibrary.com.]

If n is between 0.1 and 1, then adsorption is favorable.[32] The Langmuir and Freundlich parameters are also listed in Table III.

From the Langmuir isotherm (Fig. 13), the R^2 values for Pb^{2+}, Cu^{2+}, Co^{2+} were 0.912, 0.956, and 0.910, respectively. From the Q_o values (Table III) Pb(II) ions had the highest adsorption capacity, and the R values for all metal ions were > 0, indicating that adsorption was favorable. The Freundlich constants K_f, were calculated to be 0.041, 0.288, and 0.776 mg g^{-1} for Pb^{2+}, Cu^{2+}, Co^{2+}, respectively. The R^2 values obtained from the Freundlich isotherm plots are lower than those obtained from the Langmuir plots for all metal ions, suggesting that the adsorption data can best be modeled by the Langmuir isotherm.

Desorption and reusability studies

Desorption studies were carried out with 2*M* solutions of NaOH and HCl, and HCl was found to be more efficient. This was expected because in acidic medium, the hydronium ions in solution replaces the metal ions on the composite material while in basic medium, recovery was poor perhaps due to coordinating ligands being protonated, resulting in the

TABLE IV
Adsorption–Desorption Cycle of Pb(II) onto HCl-EVA/C (85/15)

1st Cycle		2nd Cycle		3rd Cycle		4th Cycle	
Ads	Des	Ads	Des	Ads	Des	Ads	Des
78.46	66.42	75.13	72.38	70.32	64.15	59.26	51.78

"Ads" and "Des" represent the adsorbed and desorbed amounts (%), respectively.

metal cations detached from the adsorbent material. Desorption studies for all three metal cations showed a similar trend, but Table IV shows the desorption results for Pb(II) obtained from four consecutive cycles. Although the amount adsorbed in the subsequent cycles is less than that adsorbed in the first cycle, significant amount of metal ion is removed, an indication that the material can be used reused over a significant period of time. The desorbed amounts were somewhat inconsistent, and although complete desorption could not be achieved, desorbed amounts of up to 72% (2nd cycle) were obtained. The incomplete desorption of metal cations could be attributed to interference by nonelectrostatic forces between the metal and the composite material.[32]

CONCLUSIONS

A novel EVA-C nanocomposite was successfully synthesized, and its applicability in heavy metal uptake in aqueous solutions was investigated with reference to Cu(II), Pb(II), and Co(II). The high adsorption efficiencies obtained suggest that this type of composite holds great potential for use in water decontamination, and that such removal capacity generally increases with an increasing amount of the filler. Pretreatment was found to significantly influence the overall performance of the adsorbent composite, but was dependent on the conditioning reagent. Adsorption data can best be modeled by the Langmuir isotherm rather than by the Freundlich isotherm. Re-usability studies indicate that this material possesses the potential for use over significant periods of time, although complete desorption of the metal cation from the composite material could not be achieved.

References

1. Markowitz, M. Pediatr Rev 2000, 10, 327.
2. Kopittke, P. M.; Asher, C. J.; Kopittke, R. A.; Menzies, M. W. Environ Pollut 2007, 150, 280.
3. Agency for Toxic Substances and Disease Registry (ATSDR). Draft Toxicological Profile for Cobalt. US Department of Health and Human Services; Atlanta, G. A, 2001.
4. Quing, D. Alternative Med Rev 1998, 3, 262.
5. Fierro, V.; Torne-Fernandez, V.; Montane, D.; Celzard, A. Microporous Mesoporous Mater 2008, 111, 276.
6. Ricordel, S.; Taha, S.; Cisse, I.; Dorange, G. Sep Purif Technol 2001, 24, 389.
7. Babel, S.; Kurniawan, T. A. J Hazard Mater 2003, B97, 219.
8. Rozic, M.; Cerjan-Stefanovic, S.; Kurajica, S.; Vanica, V.; Hodzic, E. Water Res 2000, 34, 3675.
9. Farkas, A.; Rozic, M.; Barbaric-Mikocevic, Z. J Hazard Mater B 2005, 117, 25.
10. Mugan, C.; Melek, Y. Sep Purif Technol 2004, 37, 93.
11. Semmens, M. J.; Martin, W. P. Water Res 1997, 31, 1379.
12. Kesraoui-Ouki, S.; Cheeseman, C.; Perry, R. Environ Sci Technol 1993, 27, 1108.
13. Ulusoy, U.; Simsek, S. J Hazard Mater 2005, B127, 163.
14. Tsitsishvilli, G. V.; Andronikashvili, T. G.; Kirov, G. M.; Filizova, L. D. Natural Zeolites; Ellis Horwood: Chichester, West Sussex, England, 1992.
15. Inglezakis, V. J.; Grigoropoulou, H. J Hazard Mater 2004, B112, 37.
16. Kuronen, M.; Weller, M.; Townsend, R.; Harjula, R. React Funct Polym 2006, 66, 1350.
17. Hernandez, M. A. J Porous Mater 2000, 7, 443.
18. Anirudhan, T. S.; Suchithra, P. S.; Rijith, S. Colloids Surfaces A Physicochem Eng Aspects 2008, 326, 147.
19. Madejova, J. Vibrat Spectrosc 2003, 3, 1.
20. Amarasinghe, B. M. W. P. K.; Williams, R. A. Chem Eng J 2007, 132, 299.
21. Athanasiadis, K.; Helmreich, B. Water Res 2005, 39, 1527.
22. Cincotti, A.; Lai, N.; Orru, R.; Cao, G. Chem Eng J 2001, 84, 275.
23. Ederm, E.; Karapinar, N.; Donat, R. J Colloid Interface Sci 2004, 280, 309.
24. Zou, W.; Han, R.; Chen, Z.; Jinghua, Z.; Shi, J. Colloids Surfaces A Physicochem Eng Aspects 2006, 279, 238.
25. Gunay, A.; Arslankaya, E.; Tosun, I. J Hazard Mater 2007, 146, 362.
26. Barthomeuf, D. Stud Surface Sci Catal 1997, 105, 1677.
27. Bosso, S. T.; Enzweiler, J. Water Res 2002, 36, 4795.
28. Taty-Costodes, V. C.; Fauduet, H.; Porte, C.; Delacroix, A. J Hazard Mater B 2003, 105, 121.
29. Wang, Y. H.; Lin, S. H.; Juang, R. S. J Hazard Mater B 2003, 102, 291.
30. Nyembe, D. W.; Mamba, B. B.; Mulaba-Bafubiandi, A. F. J Appl Sci 2010, 10, 8.
31. Singh, K. K.; Talat, M.; Hasan, S. H. Bioresource Technol 2005, 97, 125.
32. Singh, V.; Tiwari, S.; Sharma, A. K.; Sanghi, S. J Colloid Interface Sci 2007, 316, 224.